

---

# **Time Domain Measurements using Vector Network Analyzer ZVR**

---

Application Note 1EZ44\_0E

Subject to change

19 May 1998, Olaf Ostwald

Products:

**ZVR with option ZVR-B2**

**ZVC with option ZVR-B2**

**ZVRE with option ZVR-B2**

**ZVCE with option ZVR-B2**

**ZVRL with option ZVR-B2**



**ROHDE & SCHWARZ**

CONTENTS	PAGE
1 ABSTRACT	2
2 TYPICAL APPLICATION	2
3 THEORY	4
3.1 IMPULSE AND STEP RESPONSES	4
3.2 FINITE PULSE WIDTH	7
3.3 ALIASING	8
3.4 BANDPASS AND LOWPASS MODE	9
4 WINDOWS	10
5 GATES	12
6 MEASUREMENT EXAMPLES	13
6.1 STEPPED AIRLINE	13
6.2 FAST MEASUREMENTS	14
7 REFERENCES	15
7.1 ON TIME DOMAIN TRANSFORM	15
7.2 ON VECTOR NETWORK ANALYZER	15
FAMILY ZVR	15
8 ORDERING INFORMATION	15
9 ANNEX	16
9.1 TIME DOMAIN REPRESENTATIONS	16
9.2 SPECTRA OF FILTER FUNCTIONS	16

## 1 ABSTRACT

Vector Network Analyzers of the ZVR family are able to measure magnitude and phase of complex S-parameters of a device under test (DUT) in the frequency domain. By means of the inverse Fourier transform the measurement results can be transformed to the **time domain**. Thus, the **impulse** or **step response** of the DUT is obtained, which gives an especially clear form of representation of its characteristics. For instance, faults in cables can thus be directly localized. Moreover, special time domain filters, so-called **gates**, are used to suppress unwanted signal components such as multireflections. The measured data "gated" in the time domain are then transformed back to the frequency domain and an S-parameter representation without the unwanted signal components is obtained as a function of frequency. As usual, other complex or scalar parameters such as impedance or attenuation can then be calculated and displayed.

## 2 TYPICAL APPLICATION

As a typical example, fig. 2 shows results of a reflection measurement in the time domain. The DUT (Fig. 1) consists of a power splitter. A short-circuited 270 mm long coaxial cable is connected to one output of the power splitter, and another coaxial line with an electrical length of approx. 2750 mm is connected to the other output. The end of this cable is left open-ended in the first case (case **Open**).

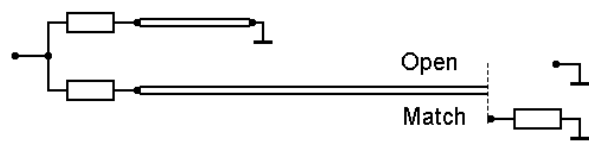


Fig. 1 DUT

Fig. 2 shows two main reflections (pulses with highest amplitudes) caused by the two total-reflecting line ends. Other smaller pulses can also be seen. They are caused by multireflections between the power splitter (12 dB mismatched at each output) and the line ends.

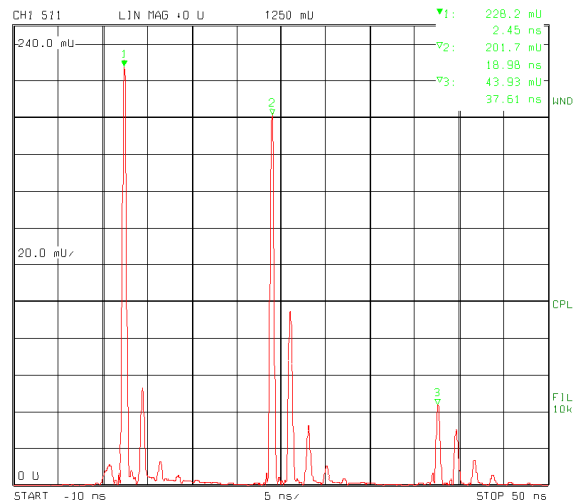


Fig. 2 Example of a reflection measurement in time domain (impulse response)

The measurement results in the frequency domain are represented by the trace shown in Fig. 3. In contrast to the time domain in which the representation is simple and clear and the different signal components can be easily distinguished, the trace in the frequency domain is obviously not easy to interpret.

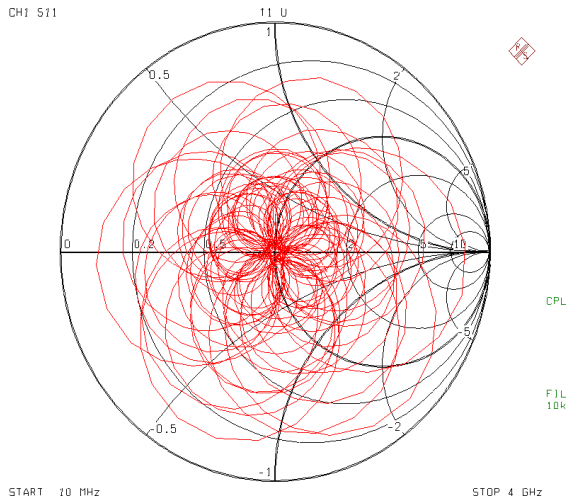


Fig. 3 Measurement results in frequency domain

Any interesting reflection can be selectively removed by means of a **gate**, i.e. a **filter in the time domain**. Such a reflection might for example be the second-highest pulse (MARKER  $\nabla 2$  in vicinity of the center of Fig. 2) resulting from the total reflection at the open end of the longer cable. The impulse response filtered in the time domain by a suitable gate (gate center = 19 ns and gate span = 1.5 ns) is shown in Fig. 4. As can be seen, all other pulses but the interesting one are suppressed by the gate.

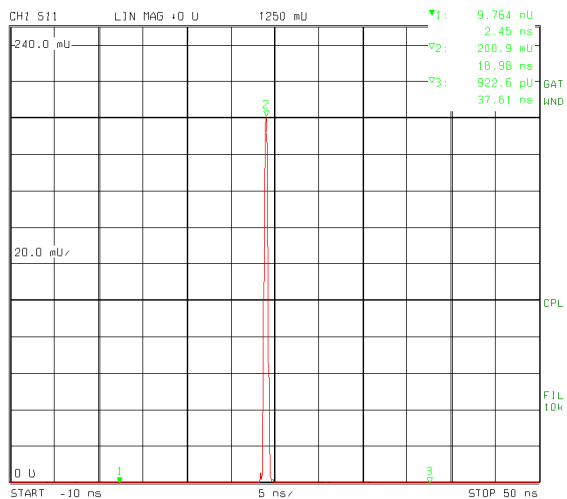


Fig. 4 Measurement results in time domain with active gate

If, in the next step, the gated impulse response is transformed back to the frequency domain, a frequency response (see Fig. 5) will be displayed, which is only representing the transfer function (in reflection) of the power splitter and the open ended cable.

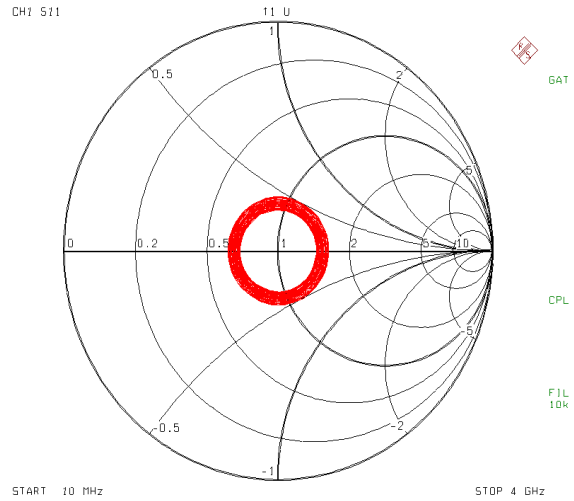


Fig. 5 Measurement results in frequency domain after time domain filtering (gating)

Now, as an experiment, the open-ended cable is terminated by a matched load (Fig. 1: case **Match**). The diagram in Fig. 6 shows the really impressive measurement results which are obtained despite of the numerous reflections of the test setup. Again, the **gated frequency response** of the DUT is displayed. Corresponding to the low reflection of the matched load used, the trace is in immediate vicinity of the center point of the Smith chart. The scaling value of the outer circle of the enlarged section around the center of the Smith chart is -20 dB. The measured values are less than -42 dB.

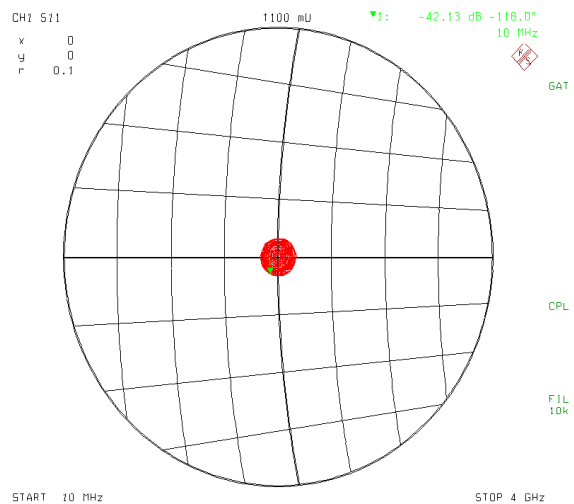


Fig. 6 Measurement results in the frequency domain with active time gate. DUT of Fig. 1 with matched load at the end of the long cable.

### 3 THEORY

Each linear and time invariant network can alternatively be represented in the time domain by its **impulse response**  $h(t)$  or in the frequency domain by its transfer function  $H(f)$ . The relation between the two forms of representation is given by the **Fourier Transform** as follows:

$$H(f) := \int_{-\infty}^{\infty} h(t) \cdot e^{-j \cdot 2 \cdot \pi \cdot f \cdot t} dt \quad (1)$$

Via Fourier transform, the impulse response is transformed to the spectral representation of the network in the frequency domain. The other way round, the data measured in the frequency domain by the network analyzer can be transformed to the time domain using **Inverse Fourier Transform**.

$$h(t) := \int_{-\infty}^{\infty} H(f) \cdot e^{j \cdot 2 \cdot \pi \cdot f \cdot t} df \quad (2)$$

The **step response** can be obtained by integration of the impulse response  $h(t)$ . Fig. 7 shows the step response for the DUT in Fig. 1.

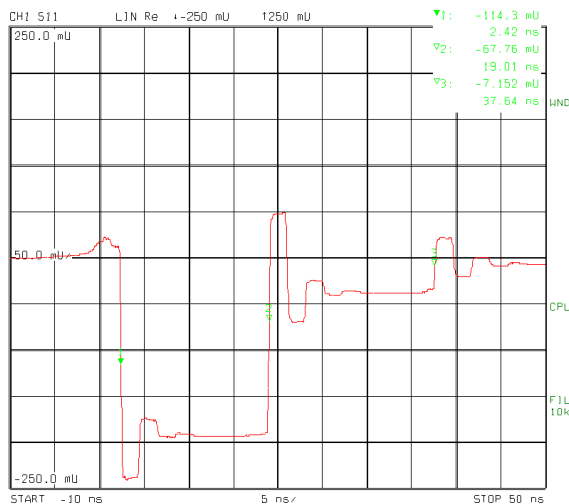


Fig. 7 Step response

This form of representation clearly shows the variation of the impedance along the DUT. The zero line in the middle of the diagram indicates zero reflection, thus representing the reference

impedance  $Z_0$ . Positive values stand for higher impedances than the reference impedance ( $Z > Z_0$ ) and negative values for lower impedances ( $Z < Z_0$ ). In general, the relationship between the measured reflection coefficient  $S_{11}$  and the impedance  $Z$  is as follows:

$$S_{11} := \frac{Z - Z_0}{Z + Z_0} \quad (3)$$

The operation sequence for the desired representation in the time domain is

**[MODE] TIME DOMAIN: DEF TRANSF TYPE.**

In the menu one can select between the impulse response (IMPULSE) and the step response (STEP).

#### 3.1 IMPULSE AND STEP RESPONSES

As already mentioned in the previous section the impulse response and step response offer different advantages for the representation of measurement results in the time domain. Mathematically, these two forms of representation are equivalent. They can be converted into each other by differentiation or integration. Historically, the step response offers technical advantages since it is easier to generate a single steep edge, i.e. a voltage **step** than two voltage steps one after the other within a very short time interval, i.e. a voltage **impulse**. This advantage, however, is superseded by the possibility to measure the transfer function of the DUT first in the frequency domain and to transform it then to the time domain in quasi-real-time. The effort required for the numerical calculation of the two forms of representation is about the same if a sufficiently fast processor is used.

It is recommended to use the step response if the impedance characteristics of the DUT are of interest. The impulse response, however, should be made use of in the most of other cases, especially for the determination of discontinuities. A further advantage of the impulse response is that in contrast to the step response its magnitude can always be sensibly interpreted even if bandpass mode is used. This will be further dealt with in section 3.4 *Bandpass and Lowpass Mode*.

The following diagrams (Figs 8 to 11) are examples of the impulse and step responses of typical DUTs (starting with an open, via different resistive loads till a short circuit). In each diagram, the **impulse response** is displayed in the **upper part** and the **step response** in the **lower part** with the same scaling.

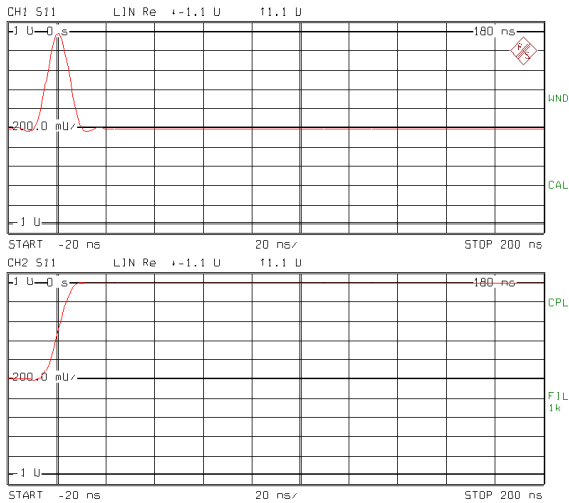


Fig. 8 Impulse and step response of an open (LOWPASS DC S-PARAM = 1)

The lowpass mode (see section 3.4) was used in all figures. For a correct representation of the step response in the lowpass mode the DC-value of the displayed S-parameter is of importance. This value can be entered using the following sequence: **[MODE] TIME DOMAIN: DEF TRANSF TYPE: LOWPASS DC S-PARAM.**

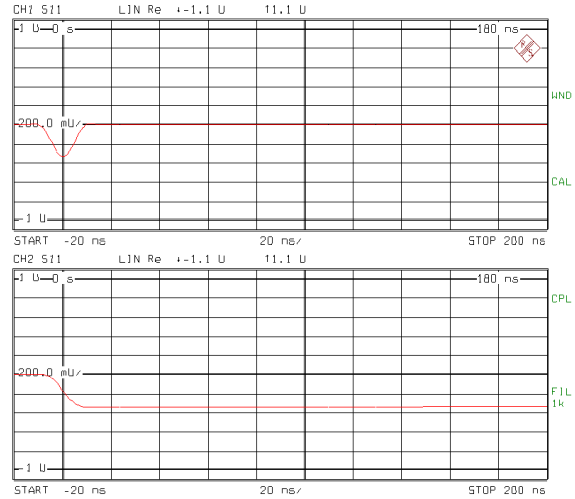


Fig. 10 Impulse and step response of a 25  $\Omega$  resistor (LOWPASS DC S-PARAM = -1/3)

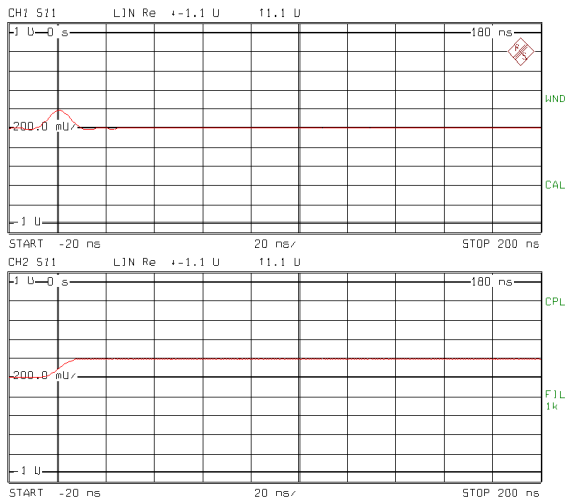


Fig. 9 Impulse and step response of a 75  $\Omega$  resistor (LOWPASS DC S-PARAM = 0.2)

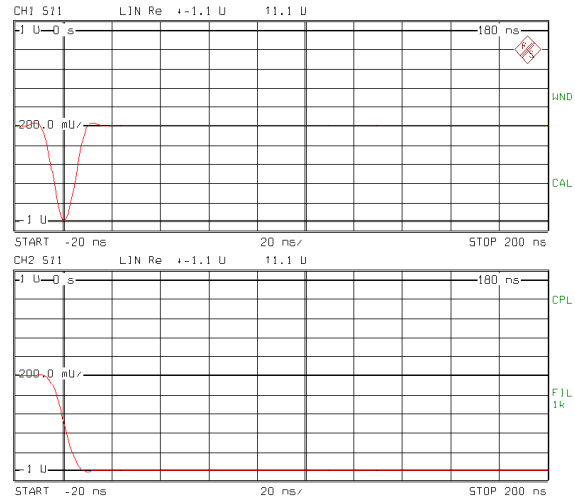


Fig. 11 Impulse and step response of a short (LOWPASS DC S-PARAM = -1)

The impulse and step response characteristics of **complex impedances** are highly interesting. The measurement results shown in the following diagrams (Figs 12 to 17) were obtained with single inductors and capacitors grounded at one end (Figs 12 and 13), and with the series (Figs 14 and 15) or parallel connection (Figs 16 and 17) of an inductor or a capacitor respectively, with a 50 Ω resistor.

For a qualitative **interpretation** of the measured responses it is useful to first illustrate the **step response**: at the very beginning of a step only the high-frequency behavior of the DUT affects the step response due to the steepness of the step. Thus at the first moments of a step stimulus a capacitor reacts similar as a through connection, whereas an inductor first appears as an interruption.

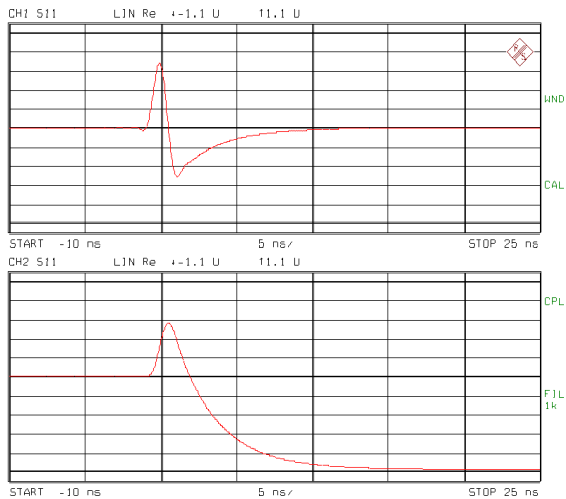


Fig. 12 Impulse and step response of a 150 nH inductor (LOWPASS DC S-PARAM = -0.97)

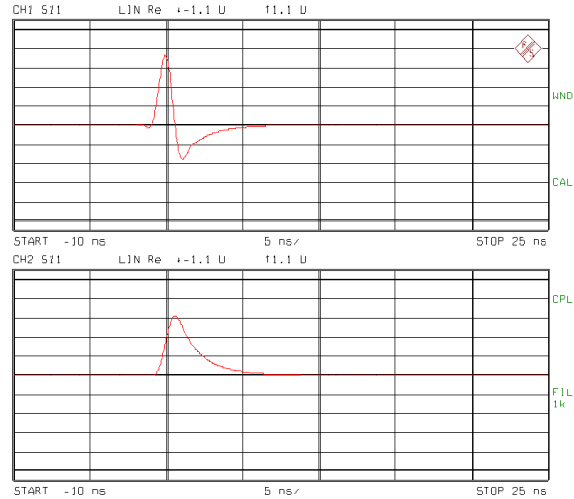


Fig. 14 **Series L**  
Impulse and step response of series connection of a 150 nH inductor and a 50 Ω resistor (LOWPASS DC S-PARAM = 0)

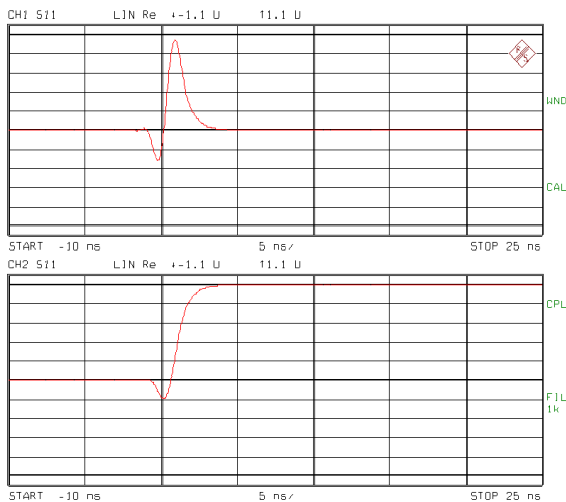


Fig. 13 Impulse and step response of a 15 pF capacitor (LOWPASS DC S-PARAM = 1)

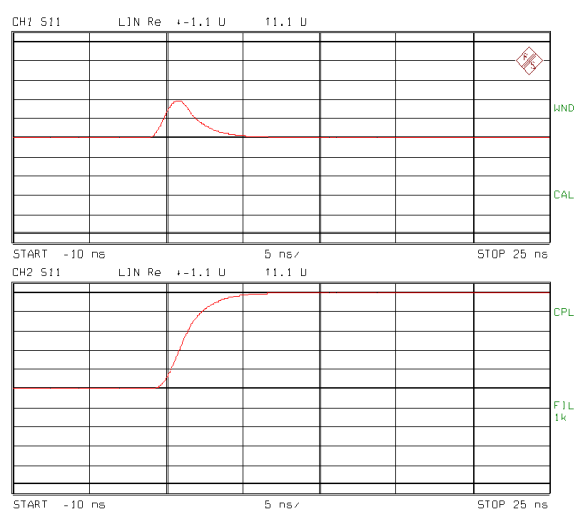
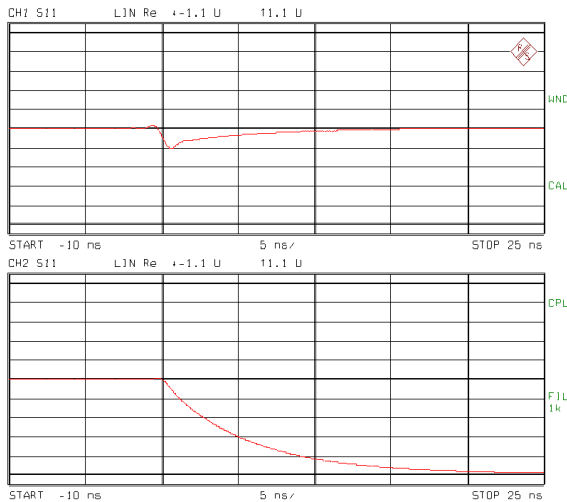
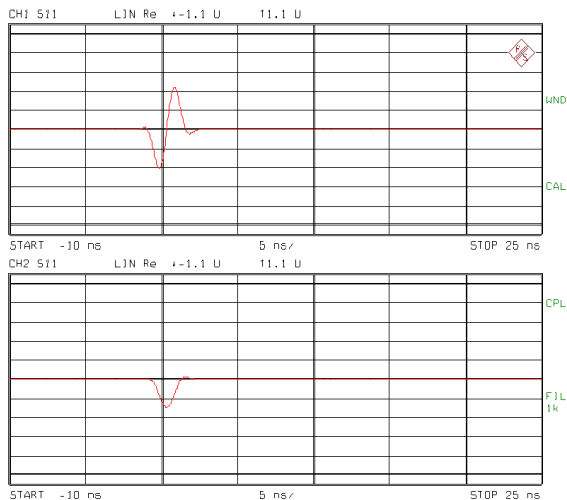


Fig. 15 **Series C**  
Impulse and step response of series connection of a 15 pF capacitor and a 50 Ω resistor (LOWPASS DC S-PARAM = 1)

The signal components of the step response occurring later in time correspond to lower and lower frequency components down to DC. Thus only the low-frequency behavior of the DUT has an effect on the later part of the step response. A capacitor now reacts like an interruption whereas an inductor for low frequencies is similar to a direct a through connection.



**Fig. 16 Parallel L**  
Impulse and step response of parallel connection of a 150 nH inductor and a 50 Ω resistor  
(LOWPASS DC S-PARAM = -1)



**Fig. 17 Parallel C**  
Impulse and step response of parallel connection of a 15 pF capacitor and a 50 Ω resistor  
(LOWPASS DC S-PARAM = 0)

A typical example is the previous measurement (Fig. 17 Parallel C: lower diagram). The characteristic of the measured step response can be explained as follows: first the capacitor acts as a short and is responsible for the negative edge of the step response. (Negative signal components of the step response signify low-impedances.) With time, the capacitor charges up and more and more acts as an open. The parallel connection consisting of capacitor and resistor is then equivalent to a single resistor. Since the value of the resistor in the example is equal to the reference impedance ( $R = Z_0$ ), no reflection will occur due to the matching. Thus the step response again attains zero.

The characteristic of the impulse response (Fig. 17: upper diagram) can be imagined by a differentiation of the step response.

To correctly interpret the measurement results displayed in the time domain by the network analyzer note that due to

- finite span and
- frequency-discrete measurement

of the network analyzer neither ideal (Dirac) impulses nor ideal (rectangular) steps can be represented.

### 3.2 FINITE PULSE WIDTH

The **limited span** of the network analyzer (e.g. ZVR with  $f_{MAX} = 4$  GHz) **widens the pulses in the time domain**. Mathematically, this behavior can be explained as follows: first, an infinitely wide frequency range is assumed. Now in fact, via Fourier transform, infinitely narrow Dirac pulses can be obtained. Because of the actual finite frequency span, the frequency domain data are multiplied by a rectangular weighting function which takes the value 1 for the actual frequency range (e.g. 9 kHz to 4 GHz) of the network analyzer and which is otherwise zero. This multiplication in the frequency domain corresponds to a convolution of ideal Dirac pulses with an si function in the time domain.

$$\text{si}(x) := \frac{\sin(x)}{x} \quad (4)$$

The **width  $\Delta T$  of the si impulses** is inversely proportional to the span  $\Delta F$  of the frequency range:

$$\Delta T := \frac{2}{\Delta F} \quad (5)$$

For a span of, say, 4 GHz the pulse is widened to approx. 500 ps as can be observed in the following diagram (Fig. 18).

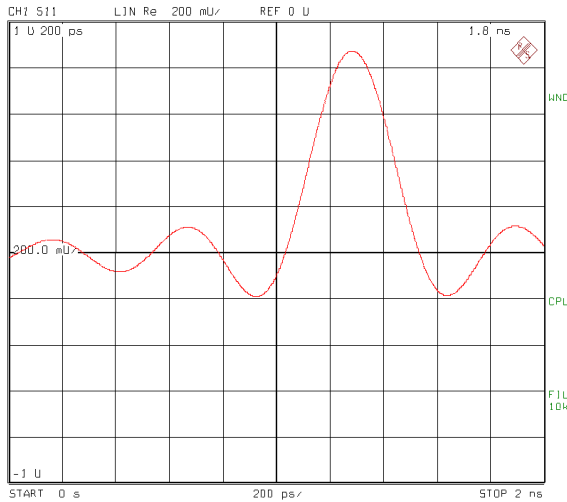


Fig. 18 Widened si impulse due to finite span (e.g.  $\Delta F = 4$  GHz).  
The pulse width  $\Delta T$  is approx. 500 ps.

Besides a widened pulse, Fig. 18 shows another characteristic of si pulses which are perceived as interference in practice: i.e. the occurrence of **ringing** (side lobes) to the left and right of the (main) pulse. According to the si function the highest (negative) side amplitudes to the left and right of the main pulse are as follows:

$$\frac{\sin\left(3 \cdot \frac{\pi}{2}\right)}{3 \cdot \frac{\pi}{2}} = -0.212 \quad (6)$$

This corresponds to a side lobe suppression of only 13.46 dB. The side lobes can be reduced by suitable **weighting methods in the frequency domain** that are also called **profiling or windowing**. For more details see section 4.

### 3.3 ALIASING

The data in frequency domain are not measured continuously versus frequency but only at a finite number of **discrete frequency points**. This causes the time domain data after transformation to be **repetitively replicated**. This phenomenon is called **aliasing** and can be explained as follows:

The frequency discrete measurements can assumed to be derived from an ideally continuous spectrum, which is multiplied by a comb spectrum in the frequency domain. In the time domain this corresponds to a convolution of the time response with a periodic Dirac impulse sequence. This results in the aliasing effect of a frequently repetition of the original time response. The representation in the time domain will thus become **ambiguous**. The time interval  $\Delta t$  between the repetitions in the time domain is called the **ambiguity range**. It can be calculated from the frequency step width  $\Delta f$  in the frequency domain as  $\Delta t = 1/\Delta f$ . This relationship is illustrated in the following diagram (Fig. 19).

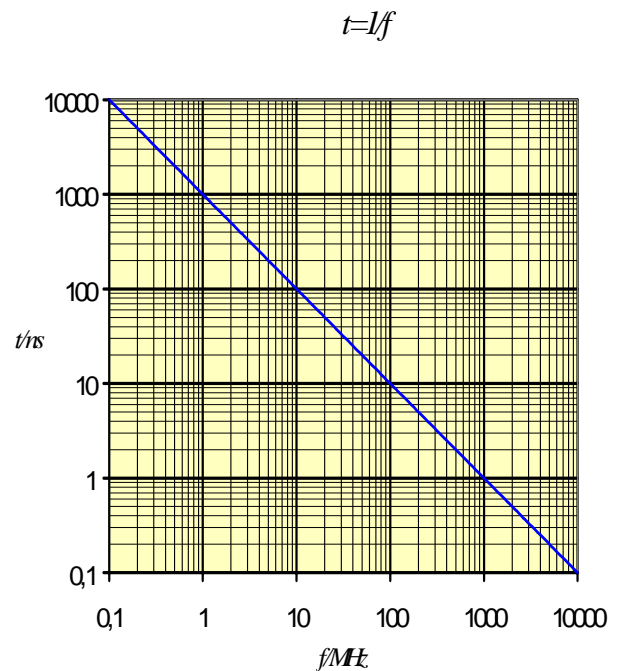


Fig. 19 Relationship between frequency step width  $\Delta f$  and ambiguity range  $\Delta t$ , or between span  $\Delta F$  and width  $\Delta T$  of pulses



For example, with the full frequency range of ZVR of 4 GHz and 400 measurement points used, the frequency step width is approximately 10 MHz. An aliasing signal such as illustrated in Fig. 20 is thus obtained every  $\Delta t = 100$  ns.

By the way, the previous diagram of Fig. 19 can also be used to convert for the relationship between  $\Delta F$  (SPAN) described above (Eq. 5) and the resulting widening  $\Delta T$  of the pulses in the time domain.

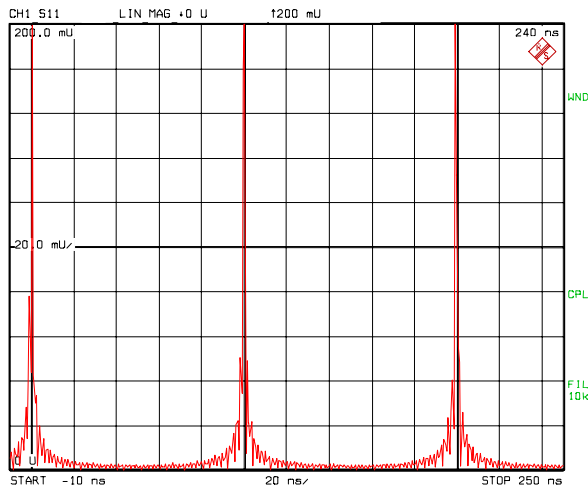


Fig. 20 Example of aliasing. The ambiguity range is  $\Delta t = 100$  ns

In Fig. 20, time domain signals can only be clearly assigned within the **ambiguity range** of  $\Delta t = 100$  ns.

If a wider ambiguity range  $\Delta t$  is required, the frequency points have to be arranged in a more dense frequency grid  $\Delta f$ . For that, either the SPAN  $\Delta F$  can be reduced by which however the time domain resolution is affected, or the NUMBER OF POINTS can be increased which reduces the measurement speed.

It should be noted that the analyzer is limited to a **maximum number of points** of 2004 for all four display channels together. The number of 2001 points is the limit per channel as it is for common measurements in the frequency domain. With the **Fast Fourier Transform** [1] used instead of the more comfortable Chirp transform [2], the number of points per channel is reduced to the next lower power-of-two number i.e. to a maximum value of 1024 points.

For the **lowpass mode** described in the following, the maximum possible number of points is halved (for the negative frequencies) and reduced by one (DC value).

### 3.4 BANDPASS AND LOWPASS MODE

Besides the default setting **bandpass mode (BANDPASS)** the network analyzer also offers the lowpass mode (LOWPASS). The bandpass mode is generally recommended for scalar applications. It allows an arbitrary number of points and an arbitrary frequency range and it is suitable to display the magnitude of the impulse response. It does however not provide any information about the measured values at zero frequency, i.e. DC value, and the spectrum is limited to positive frequencies only. As a consequence, the **impulse and step responses are therefore complex** and their phases thus depend upon the distance between the DUT and the reference plane. This has to be considered when the real or imaginary part is displayed in the time domain. It is therefore generally not recommended to use the bandpass mode when the sign of the measured reflection coefficient is of interest. The lowpass mode is required for this purpose.

In the **lowpass mode (LOWPASS)**, the frequency grid is arranged such that an exact extrapolation to zero frequency is possible. This is based on the condition that the step width  $\Delta f$  between the frequency points in the frequency domain is equal to the START frequency  $f_{START}$ , in other words:

$$f_{START} = \Delta f \quad (7)$$

A frequency grid meeting this requirement (7) is called a **harmonic grid** since the frequency value at each frequency point is an integer multiple of the START frequency. (Often, the following more general definition is used: START frequency  $f_{START}$  should be an integer multiple  $n$  of the step width  $\Delta f$ , i.e.  $f_{START} = n \cdot \Delta f$ . For the network analyzers of the ZVR family the more stringent definition with  $n=1$  is valid.)

The network analyzer is able to create a harmonic grid automatically by using the function SET FREQS LOWPASS. For further information about this topic please refer to the operating manual.

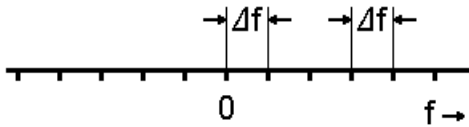


Fig. 21 Lowpass grid

After generation of the required harmonic grid, the network analyzer is able

1. to add an additional frequency point at zero frequency (DC value) to the frequency grid and
2. to mirror the data measured at positive frequencies around zero frequency to the negative frequencies in a conjugate complex way.

In the lowpass mode the width of the frequency domain is thus doubled (see Fig. 21) and in contrast to the bandpass mode the resolution in the time domain is improved by the factor of two for the step response as well as for the impulse response. Furthermore a **real time response** (imaginary part = 0) is obtained. Compared to Fig. 18 the pulse in Fig. 22 is clearly narrower. The two diagrams have an identical scaling. The figure shows the width of the si pulse reduced by the factor of two which is now only 250 ps instead of 500 ps.

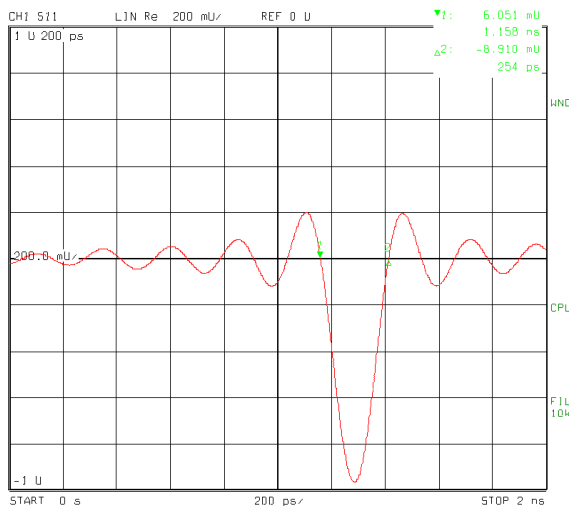


Fig. 22 Width of si pulse ( $\Delta F = 4$  GHz) halved in lowpass mode in comparison with Fig. 18. The pulse width  $\Delta T$  is now approx. 250 ps.

Besides the reduction of the pulse width the pulse in Fig. 22 has a negative amplitude in contrast to Fig. 18. Since the DUT was in both cases a shorted line ( $S_{11} = -1$ ), the measured negative amplitude of Fig. 22 fully complies with the expectations whereas Fig. 18 needs to be afterwards explained: The reason for the apparently incorrect amplitude of Fig. 18 has already been given above. It is due to the relationship between the **bandpass mode and its complex time response**. For that the phase of the time response becomes delay-dependent, which corresponds to alternating amplitudes of the real and imaginary parts. The **lowpass mode** on the other hand provides a **real time response** (imaginary part = 0) and thus always the correct sign and amplitude of the reflection coefficient of the shorted line end.

#### 4 WINDOWS

As already described in section 3.2 the pulses in the time domain are widened as a result of the limited frequency range and ringing occurs (side lobes). Especially the latter is disadvantageous for time domain measurements since fraudulent echos may be originated and the resolution as well as measurement accuracy impaired.

Suitable **windowing** (also called: profiling) the measured frequency domain data is considered to be a remedy. Windowing is essentially an attenuation of spectral components in the vicinity of the START and STOP frequencies. For that, the analyzer offers different **windows** [3] that are listed in the following table (TABLE 1).

Frequency domain <b>Window</b>	Time domain <b>Gate</b>	Filter function
NO PROFILING	STEEPEST EDGES	Rectangle
LOW FIRST SIDELOBE	STEEP EDGES	Hamming
NORMAL PROFILE	NORMAL GATE	Hann
STEEP FALLOFF	MAXIMUM FLATNESS	Bohman
ARBITRARY SIDELOBES	ARBITRARY GATE SHAPE	Dolph-Chebichev

TABLE 1 Filter functions for available windows and gates

Depending on the selected window (profile) the shape of the time domain impulses (and time domain steps) are influenced differently. This is illustrated in the following figures. In the quad channel quad split display below, Fig. 23 shows the measured reflection of an OPEN standard directly connected to PORT 1 of the network analyzer. NO PROFILING was used in channel 1 (top left). In channel 2 (bottom left) a profile (window) with a LOW FIRST SIDELobe was selected. The NORMAL PROFILE recommended for general applications was used in channel 3 (top right), and the STEEP FALLOFF (of side lobes) window in channel 4 (bottom right).

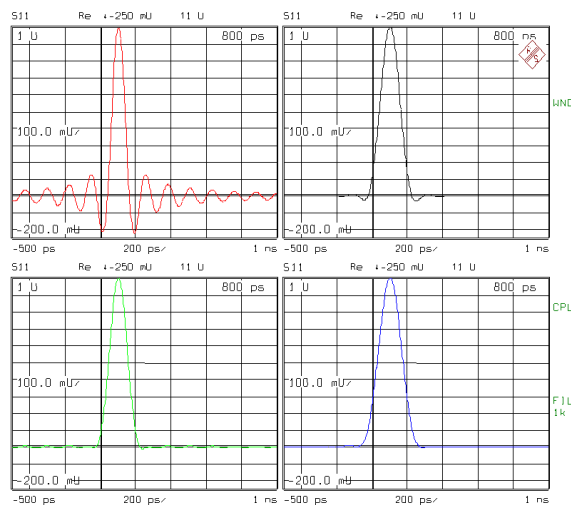


Fig. 23 Quad channel quad split display of impulses with different windows

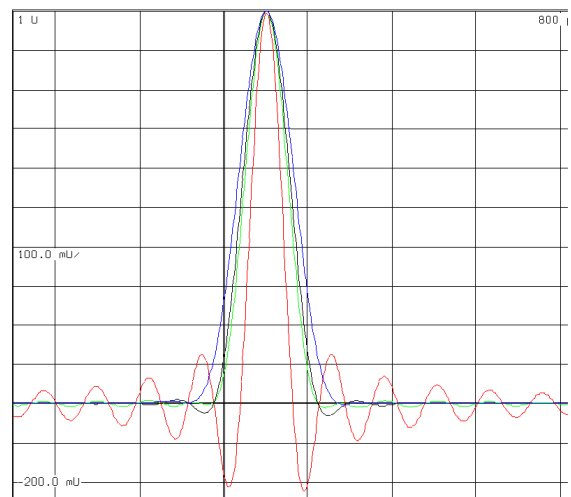


Fig. 24 Quad channel overlay display of impulses with different windows

1. **NO PROFILING** (see Fig. 23 top left or - if colored printout is available - red trace in Fig. 24) indicates that no profiling (windowing) was used. The rectangular frequency range limitation is maintained. The impulses remain si-shaped and have a relatively narrow main lobe but substantial side lobes. The highest side lobe is approx. 13 dB below the main lobe.
2. **LOW FIRST SIDELobe** (see Fig. 23 bottom left, or green trace in Fig. 24) uses the filter function according to R. W. Hamming for windowing in the frequency domain. This window yields far smaller side lobes (approx. 43 dB) than those of the rectangular window but the side lobes are hardly more attenuated even far off the main lobe. The first side lobe however is very strongly reduced. In the time domain this is indicated by a widened main lobe and clearly reduced ringing which however does not fully disappear even far from the main pulse.
3. **NORMAL PROFILE** (see Fig. 23 top right, or black trace in Fig. 24) makes use of the filter function according to Julius von Hann. In the frequency domain it is characterized by a first side lobe of approx. 32 dB, i.e. slightly higher than the Hamming filter. The other side lobes however are attenuated more strongly. This results in a visible first side lobe in the time domain even with linear scaling, but all other side lobes further away are neglectable for most applications.
4. **STEEP FALLOFF** (see Fig. 23 bottom right, or blue trace in Fig. 24) makes use of a Bohman filter which is characterized by the steepest falloff of side lobe amplitudes of all filters used. Thus, time domain pulses with practically no side lobes are obtained. The drawback is however that the pulse width is doubled compared to the rectangular window.
5. Especially high flexibility is offered by the **ARBITRARY SIDELobES** window. A filter function according to Dolph-Chebichev is used which is characterized by constant side lobe amplitudes both in the frequency and time domain. The user may select an arbitrary side lobe suppression between 10 dB and 120 dB. As for the other windows the same also applies here: high side lobe suppression is combined with wide main lobe and vice versa.

For examples see Annex.

The effects of different windows on the shape of the time domain impulses as illustrated in Figs 23 and 24 can also be observed on the display of the network analyzer itself. To do this, for example the reflection ( $S_{11}$ ) of PORT 1 of the analyzer is measured in the time domain after connecting an OPEN standard to PORT 1. The key sequence

#### [MODE] TIME DOMAIN: DEF TRANSF TYPE

calls up the menu for defining the time domain transform. By selecting one of the five possible windows (from NO PROFILING to ARBITRARY SIDELOBES) the different effects on the measured impulse or step responses can directly be observed on the display of the analyzer. Moreover, the effect of different side lobe suppressions can also be examined.

The Hann filter (NORMAL PROFILE) is recommended for most of the general applications. It is a suitable compromise between high side lobe attenuation and relatively small main lobe widening.

## 5 GATES

The TIME GATE is one of the most powerful tools of the option *Time Domain ZVR-B2*. It allows to filter out components, impedance discontinuities or line faults that are spatially separated, in the time domain. Due to the different distances to the reference plane of the network analyzer the associated **reflections** arrive at the test port at different times and can thus be measured separately from each other in the time domain. For **transmission measurements** direct transmissions can be distinguished in the time domain from indirect transmissions (multipath), i.e. multireflected transmissions (triple transit) or signal components with different propagation speeds. These capabilities have already been mentioned in section 2 *Typical Application*. The real benefit of the gate function is the transformation of the impulse response of the DUT filtered in the time domain back to the frequency domain. The interesting part of the DUT can thus be displayed without unwanted discontinuities (see Figs 2 to 6).

It is important to quickly perform all required calculations so that measurement results can be displayed in virtually real time even after two Fourier transforms including time domain gating (see also section 6.2).

The relationships between frequency domain and time domain described in section 4 on windowing also apply conversely between the

time domain and frequency domain. During filtering in the time domain using gates it is therefore important to observe the **shape of the gates** besides their position and span. A rectangular gate in the time domain does not yield optimum results in the frequency domain as might have been expected. When the impulse response filtered in the time domain by a rectangular gate is transformed back, a frequency domain response is obtained which may quickly change versus frequency but whose form is falsified. This behavior is analogous to the si impulse in the time domain created by the rectangular window in the frequency domain. It has a relatively narrow main lobe with a fast cutoff rate (rapid changes can be seen) but significant side lobes (causing ripple in the frequency domain).

1. The gate with the **STEEPEST EDGES** is therefore recommended for use only if discontinuities that are very close to each other have to be separated. The drawback here is a falsified frequency domain response resulting from the high side lobe amplitudes (max. 13 dB) of a rectangular filter spectrum which causes ripple on the trace.
2. **STEEP EDGES** is a filter (according to Hamming) whose side lobe amplitudes are far smaller (43 dB) but that hardly fall off further with increasing order.
3. **NORMAL GATE** makes use of a filter according to Hann. It is a good compromise between relatively low first side lobe (32 dB), steep falloff of further side lobes, not too wide main lobe and relatively flat passband of main lobe. It is therefore recommended **for general applications**.
4. **MAXIMUM FLATNESS** is a Bohman filter with the flattest main lobe of all filters used (nearly no passband ripple) but is also the widest main lobe. The side lobes are very low. It is suitable for use if the responses to be separated are very far from each other.
5. **ARBITRARY GATE SHAPE** is a Dolph-Chebichev filter giving the same amplitude for all side lobes. The desired side lobe suppression can be chosen by the user between 10 dB and 120 dB below the main lobe. It allows individual optimization of the gate shape for especially critical measurement tasks.

The five types of time gates have already been given in TABLE 1 together with the possible windows in the frequency domain. For further information about gate shapes and their spectra see diagrams in the Annex.

## 6 MEASUREMENT EXAMPLES

### 6.1 STEPPED AIRLINE

A stepped airline comprising a section with a characteristic impedance of  $25\ \Omega$  (thickened center conductor) is an especially instructive example that is often used to verify the measurement accuracy of network analyzers. Fig. 25 shows schematically a stepped airline, which is then terminated at one end with a  $50\ \Omega$  matched load.

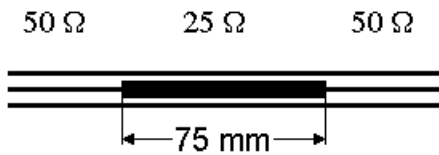


Fig. 25 Stepped airline

Impedance steps from first  $50\ \Omega$  to  $25\ \Omega$  and then from  $25\ \Omega$  to  $50\ \Omega$  cause reflections that can easily be seen in the time domain (Fig. 26). The magnitude of the reflection coefficient at the line discontinuities is 33.3% as calculated via equation (3). This corresponds to a return loss of 9.54 dB.

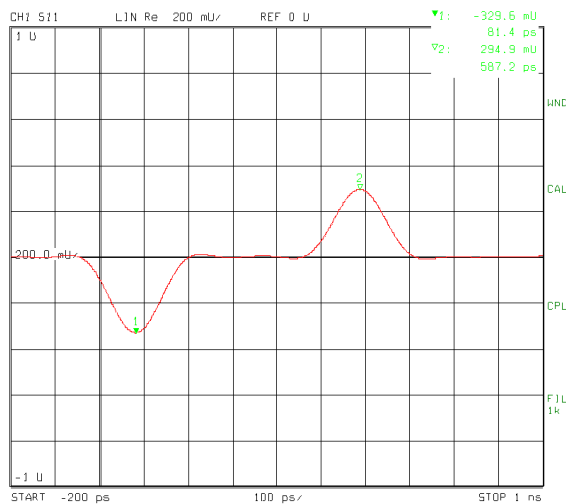


Fig. 26 Impulse response of a stepped airline

Alternatively to the impulse response, the step response can be displayed (Fig. 27). It gives a clear representation of the DUT's impedance characteristic. The measured zero of the step response can be seen in the left of the following diagram. It corresponds to the characteristic impedance of  $50\ \Omega$ . The trace then falls to the value  $-0.333$  (MARKER  $\nabla 3$ ) which exactly corresponds to the reflection coefficient expected for  $25\ \Omega$ . Then, the trace slightly increases and 500 ps later (this interval corresponds to the length of the  $25\ \Omega$  section of 75 mm) goes back again. A closer look at Fig. 27 reveals that the step response does not exactly return to the original value (zero) but only attains  $-0.04$ . This is partly due to the loss of energy (approx. 11%) of the transmitted step signal which is caused by the first line discontinuity. A further loss of energy is caused by the attenuation of the air line. Because of these two energy losses the amplitude of the step signal at the second impedance discontinuity (at the end of the  $25\ \Omega$  section) is smaller than at the beginning and the positive step in the amplitude is thus lower than the negative step at the beginning.

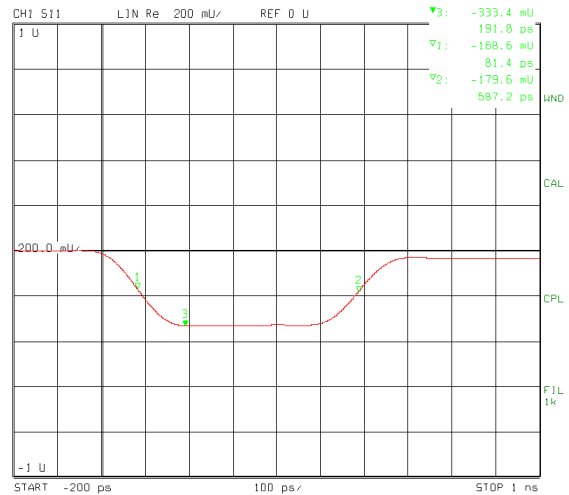


Fig. 27 Step response of stepped airline

The line attenuation can even be seen within the 25  $\Omega$  section of the airline. The central section of the trace of Fig. 27 has been enlarged. This section corresponds to the 25  $\Omega$  section of the airline and is shown in Fig. 28 with a higher resolution.

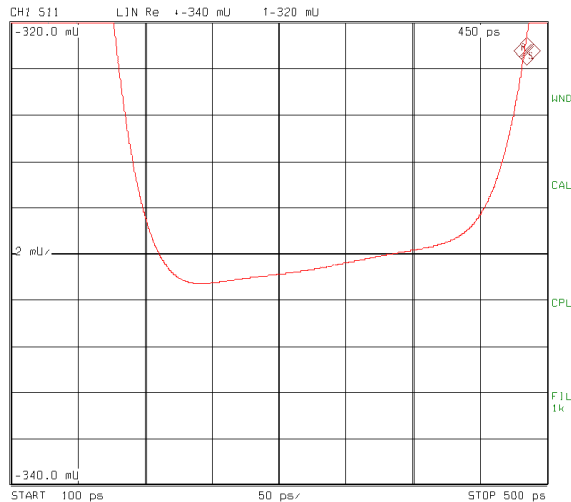


Fig. 28 Amplitude falloff of the step response due to attenuation of the airline

The Dolph-Chebichev filter (ARBITRARY SIDELOBES) with a side lobe suppression of 70 dB was selected as window in the frequency domain. A smooth trace is thus obtained that corresponds to the constant attenuation of the airline. With an unsuitable window selected, an interfering ripple of the trace would be produced.

## 6.2 FAST MEASUREMENTS

For many practical applications it is extremely important that the Fourier transform of the data measured in the frequency domain to the time domain, and the subsequent gating in the time domain, as well as the retransformation back to the frequency domain is performed fast enough for the DUT to be aligned in real time. The network analyzers of the ZVR family offer various ways for speed optimization.

It has to be noted that transformed data cannot, of course, be displayed more quickly than the data acquisition in the frequency domain is performed. Therefore, the IF BANDWIDTH has to be sufficiently high for the SWEEP TIME to be as small as desired. If required, the NUMBER OF POINTS has to be reduced to, say 100 points. To meet highest speed demands, FAST MODE in [MODE] menu should be switched on. The IF bandwidth will then automatically be switched to the maximum possible value of 26 kHz (FULL) and in addition reduced times for

the transients of the generator and receiver of the analyzer will be set.

Moreover, Fast Fourier Transform is to be selected as transformation method ([MODE] TIME DOMAIN: DEF TRANSF TYPE: FFT) since it is faster than the Chirp transform. However, with FFT all measurement points in the time domain are always evenly distributed over the ambiguity range  $\Delta t$  (= reciprocal step width  $\Delta f$  in the frequency domain). This is why the number of measurement points is reduced when a time span narrower than the ambiguity range is displayed.

On the other hand, the Chirp transform allows to set any arbitrary time span and always displays the full number of points irrespective of the ambiguity range. It is therefore more convenient to use but not as fast as FFT.

Olaf Ostwald, 1ES3  
Rohde & Schwarz  
19 May 1998

## 7 REFERENCES

### 7.1 ON TIME DOMAIN TRANSFORM

- [1] H. Marko: Methoden der Systemtheorie, Springer-Verlag, 1982.
- [2] L. R. Rabiner et al.: The Chirp z-transform Algorithm, IEEE Trans. on Audio and Electroacoustics, vol. AU-17, no.2, June 1969, pp. 86-92.
- [3] F. J. Harris: On the Use of Windows for Harmonic Analysis with Discrete Fourier Transform, Proc. of the IEEE, vol. 66, no.1, Jan. 1978, pp. 51-83.

### 7.2 ON VECTOR NETWORK ANALYZER FAMILY ZVR

- [4] O. Ostwald: 3-Port Measurements with Vector Network Analyzer ZVR, Appl. Note 1EZ26\_1E.
- [5] H.-G. Krekels: Automatic Calibration of Vector Network Analyzer ZVR, Appl. Note 1EZ30\_1E.
- [6] O. Ostwald: 4-Port Measurements with Vector Network Analyzer ZVR, Appl. Note 1EZ25\_1E.
- [7] T. Bednorz: Measurement Uncertainties for Vector Network Analysis, Appl. Note 1EZ29\_1E.
- [8] P. Kraus: Measurements on Frequency-Converting DUTs using Vector Network Analyzer ZVR, Appl. Note 1EZ32\_1E.
- [9] J. Ganzert: Accessing Measurement Data and Controlling the Vector Network Analyzer via DDE, Appl. Note 1EZ33\_1E.
- [10] J. Ganzert: File Transfer between Analyzers FSE or ZVR and PC using MS-DOS Interlink, Appl. Note 1EZ34\_1E.
- [11] O. Ostwald: Group and Phase Delay Measurements with Vector Network Analyzer ZVR, Appl. Note 1EZ35\_1E.
- [12] O. Ostwald: Multiport Measurements using Vector Network Analyzer, Appl. Note 1EZ37\_1E.
- [13] O. Ostwald: Frequently Asked Questions about Vector Network Analyzer ZVR, Appl. Note 1EZ38\_3E.
- [14] A. Gleißner: Internal Data Transfer between Windows 3.1 / Excel and Vector Network Analyzer ZVR, Appl. Note 1EZ39\_1E.
- [15] A. Gleißner: Power Calibration of Vector Network Analyzer ZVR, Appl. Note 1EZ41\_2E.
- [16] O. Ostwald: Pulsed Measurements on GSM Amplifier SMD ICs with Vector Analyzer ZVR, Appl. Note 1EZ42\_1E.

## 8 ORDERING INFORMATION

Order designation	Type	Frequency range	Order No.
<b>Vector Network Analyzers (test sets included) *</b>			
3-channel, unidirectional, 50 Ω, passive	ZVRL	9 kHz to 4 GHz	1043.0009.41
3-channel, bidirectional, 50 Ω, passive	ZVRE	9 kHz to 4 GHz	1043.0009.51
3-channel, bidirectional, 50 Ω, active	ZVRE	300 kHz to 4 GHz	1043.0009.52
4-channel, bidirectional, 50 Ω, passive	ZVR	9 kHz to 4 GHz	1043.0009.61
4-channel, bidirectional, 50 Ω, active	ZVR	300 kHz to 4 GHz	1043.0009.62
3-channel, bidirectional, 50 Ω, active	ZVCE	20 kHz to 8 GHz	1106.9020.50
4-channel, bidirectional, 50 Ω, active	ZVC	20 kHz to 8 GHz	1106.9020.60
<b>Alternative Test Sets *</b>			
<b>75 Ω SWR Bridge for ZVRL (instead of 50 Ω) <sup>1)</sup></b>			
75 Ω, passive	ZVR-A71	9 kHz to 4 GHz	1043.7690.18
<b>75 Ω SWR Bridge Pairs for ZVRE and ZVR (instead of 50 Ω) <sup>1)</sup></b>			
75 Ω, passive	ZVR-A75	9 kHz to 4 GHz	1043.7755.28
75 Ω, active	ZVR-A76	300 kHz to 4 GHz	1043.7755.29
<b>Options</b>			
AutoKal	ZVR-B1	0 to 8 GHz	1044.0625.02
Time Domain	ZVR-B2	same as analyzer	1044.1009.02
Mixer Measurements <sup>2)</sup>	ZVR-B4	same as analyzer	1044.1215.02
Reference Channel Ports	ZVR-B6	same as analyzer	1044.1415.02
Power Calibration <sup>3)</sup>	ZVR-B7	same as analyzer	1044.1544.02
3-Port Adapter	ZVR-B8	0 to 4 GHz	1086.0000.02
Virtual Embedding Networks <sup>4)</sup>	ZVR-K9	same as analyzer	1106.8830.02
4-Port Adapter (2xSPDT)	ZVR-B14	0 to 4 GHz	1106.7510.02
4-Port Adapter (SP3T)	ZVR-B14	0 to 4 GHz	1106.7510.03
Controller (German) <sup>5)</sup>	ZVR-B15	-	1044.0290.02
Controller (English) <sup>5)</sup>	ZVR-B15	-	1044.0290.03
Ethernet BNC for ZVR-B15	FSE-B16	-	1073.5973.02
Ethernet AUI for ZVR-B15	FSE-B16	-	1073.5973.03
IEC/IEEE-Bus Interface for ZVR-B15	FSE-B17	-	1066.4017.02
Generator Step Attenuator PORT 1	ZVR-B21	same as analyzer	1044.0025.11
Generator Step Attenuator PORT 2 <sup>6)</sup>	ZVR-B22	same as analyzer	1044.0025.21
Receiver Step Attenuator PORT 1	ZVR-B23	same as analyzer	1044.0025.12
Receiver Step Attenuator PORT 2	ZVR-B24	same as analyzer	1044.0025.22
External Measurements, 50 Ω <sup>7)</sup>	ZVR-B25	10 Hz to 4 GHz (ZVR/E/L) 20 kHz to 8 GHz (ZVC/E)	1044.0460.02

<sup>1)</sup> To be ordered together with the analyzer.

<sup>2)</sup> Harmonics measurements included.

<sup>3)</sup> Power meter and sensor required.

<sup>4)</sup> Only for ZVR or ZVC with ZVR-B15.

<sup>5)</sup> DOS, Windows 3.11, keyboard and mouse included.

<sup>6)</sup> For ZVR or ZVC only.

<sup>7)</sup> Step attenuators required.

**\* Note:**

Active test sets, in contrast to passive test sets, comprise internal bias networks, e.g. to supply DUTs.

## 9 ANNEX

Frequency domain <b>Window</b>	Time domain <b>Gate</b>	Filter function
NO PROFILING	STEEPEST EDGES	Rectangle
LOW FIRST SIDELOBE	STEEP EDGES	Hamming
NORMAL PROFILE	NORMAL GATE	Hann
STEEP FALLOFF	MAXIMUM FLATNESS	Bohman
ARBITRARY SIDELOBES	ARBITRARY GATE SHAPE	Dolph-Chebichev

### 9.1 TIME DOMAIN REPRESENTATIONS

Some examples of impulse responses are given. They show the reflection of an OPEN standard directly connected to PORT 1 of the network analyzer. Different windows are used:

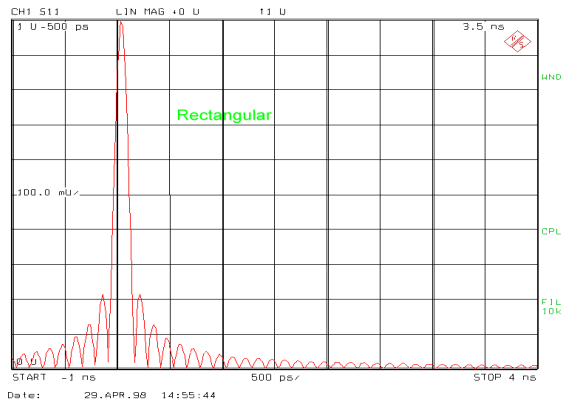
For the filter function according to Dolph-Chebichev any side lobe suppressions between 10 dB and 120 dB can be set. Values 20 dB, 40 dB, 80 dB and 120 dB are given as an example in the Annex.

### 9.2 SPECTRA OF FILTER FUNCTIONS

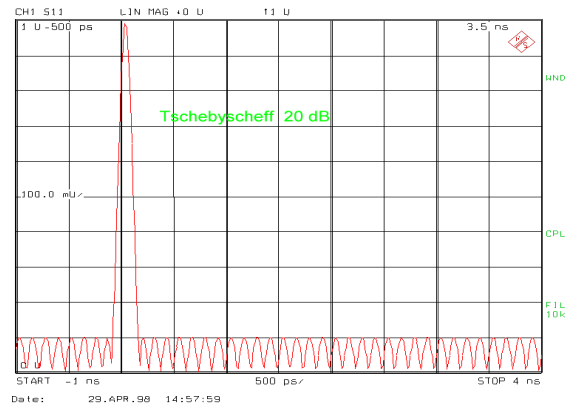
The spectra of the available filter functions are shown. Two different scalings are used. (Please ignore irrelevant abscissa labeling). The diagrams in the left column show the spectra in the vicinity of the main lobe. The right column shows the characteristic of the spectra far from the main lobe.



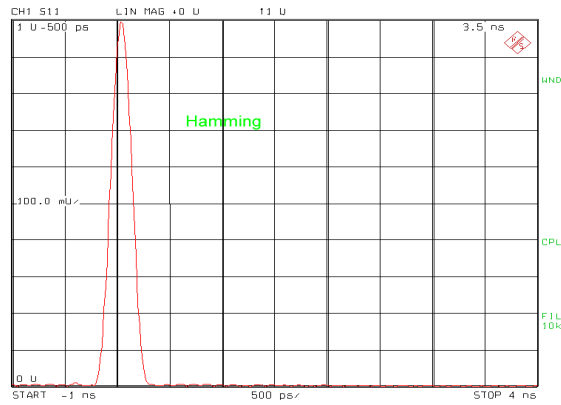
# Time Domain Representations



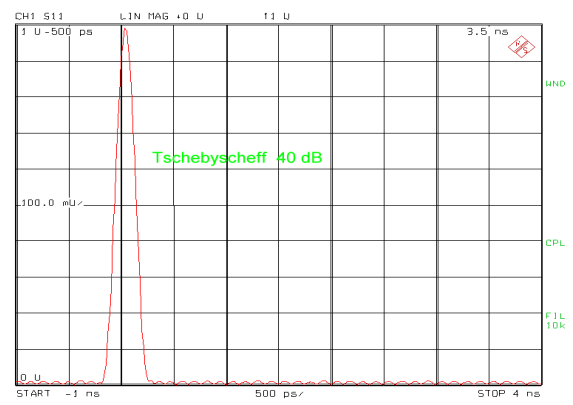
Rectangular filter



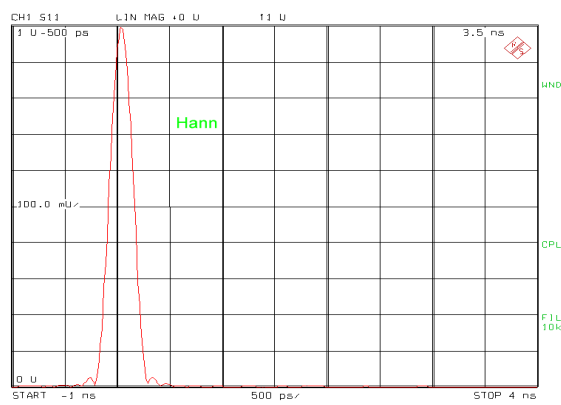
Dolph-Chebichev filter (20 dB)



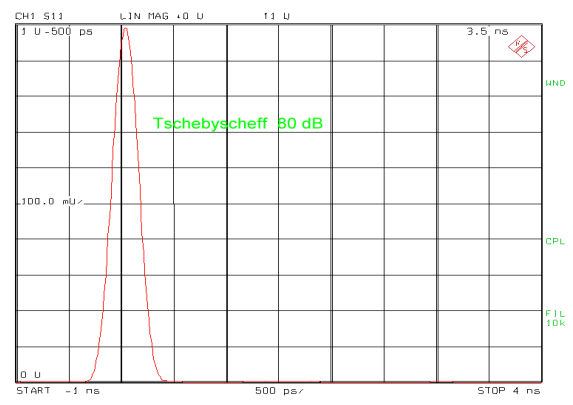
Hamming filter



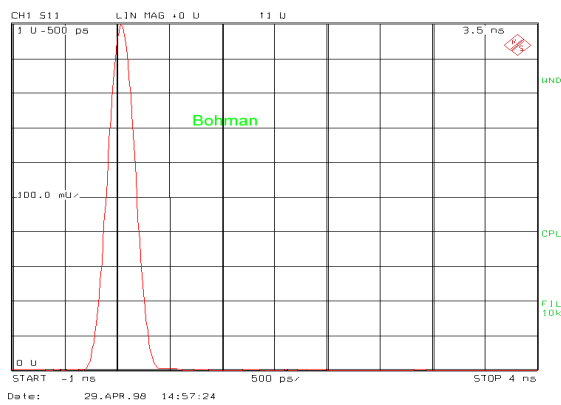
Dolph- Chebichev filter (40 dB)



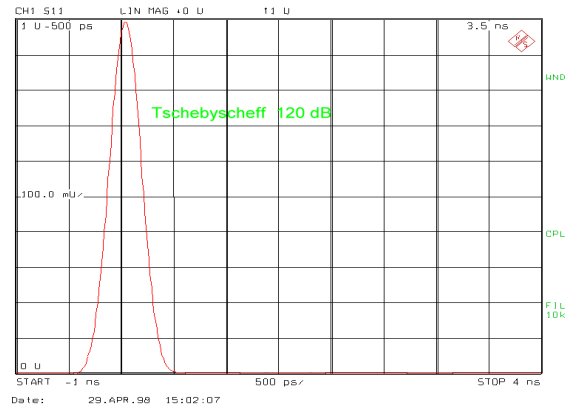
Hann filter



Dolph- Chebichev filter (80 dB)



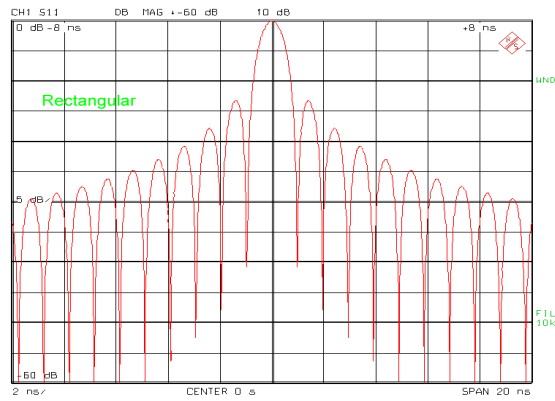
Bohman filter



Dolph- Chebichev filter (120 dB)

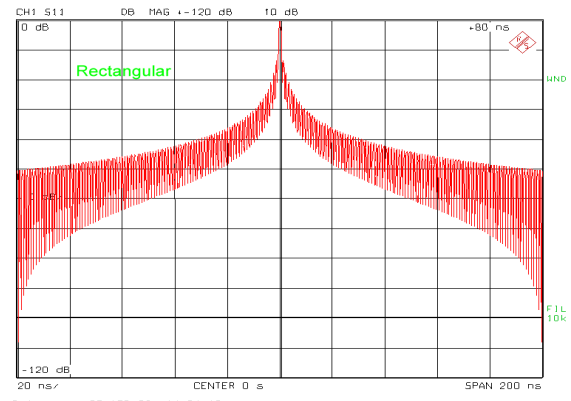
# Spectra of Filter Functions

Spectra in the vicinity of main lobe:

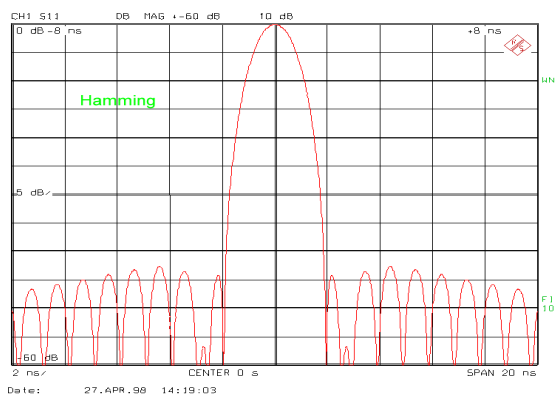


Rectangular filter

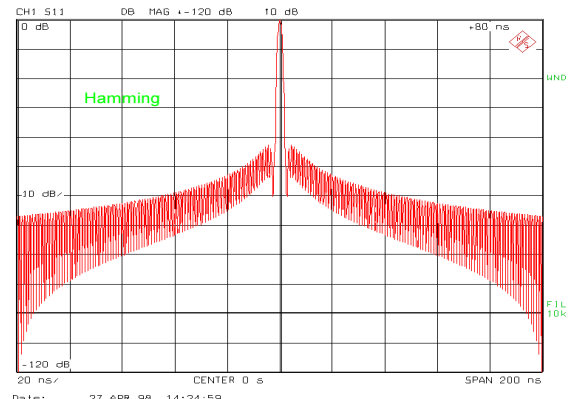
Spectra far away from the main lobe:



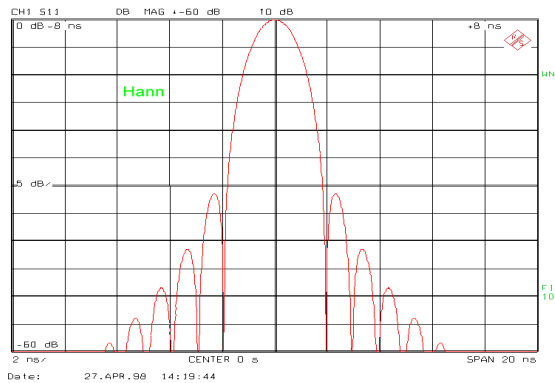
Rectangular filter



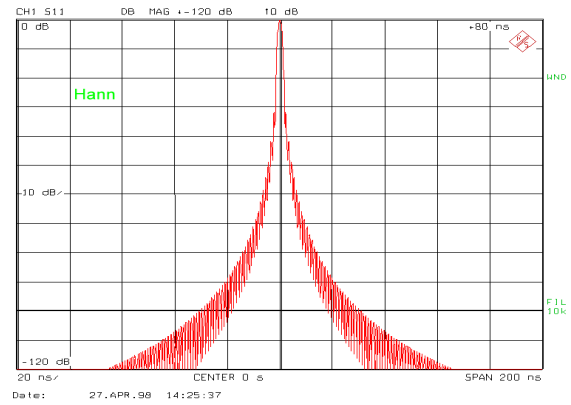
Hamming filter



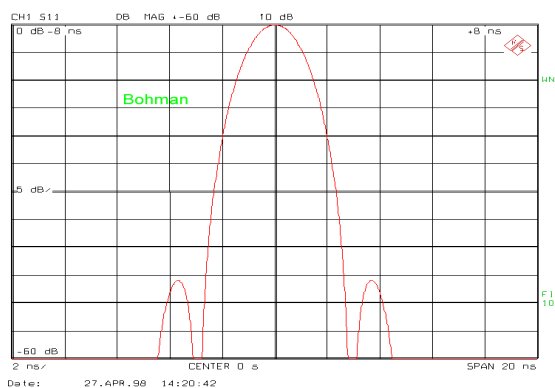
Hamming filter



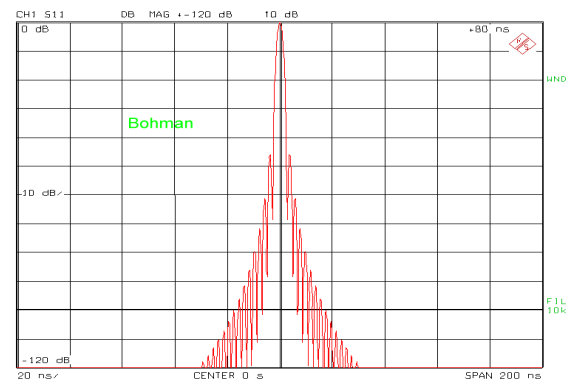
Hann filter



Hann filter



Bohman filter



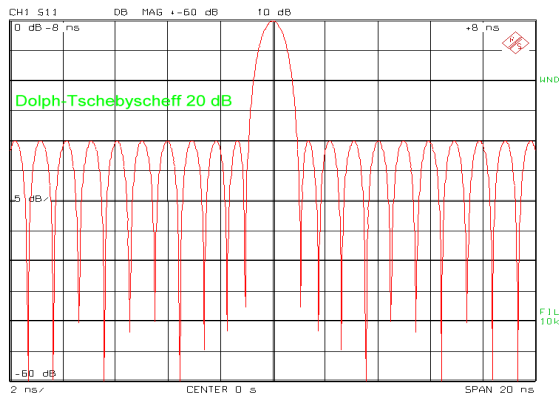
Bohman filter

# Spectra of Filter Functions:

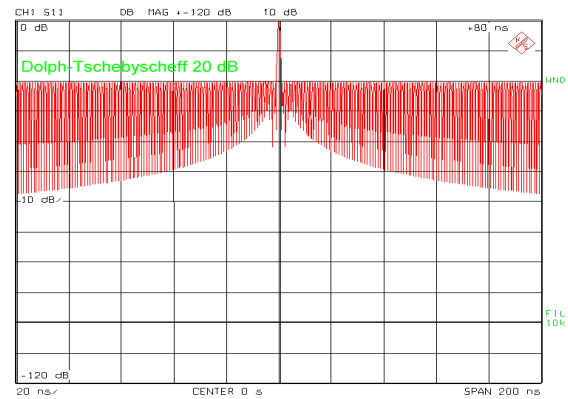
## Dolph-Chebichev filters with different side lobe suppressions

Spectra in the vicinity of main lobe:

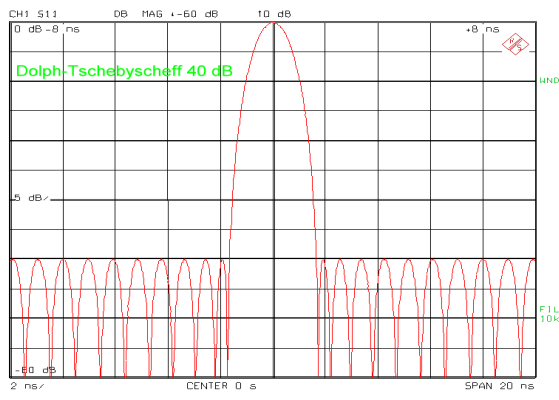
Spectra far away from the main lobe:



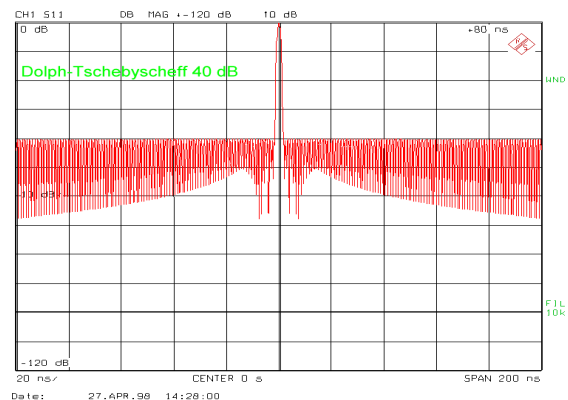
Dolph-Chebichev (20 dB side lobe suppression)



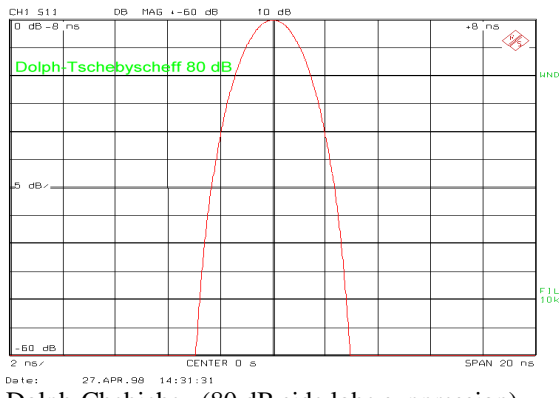
Dolph-Chebichev (20 dB side lobe suppression)



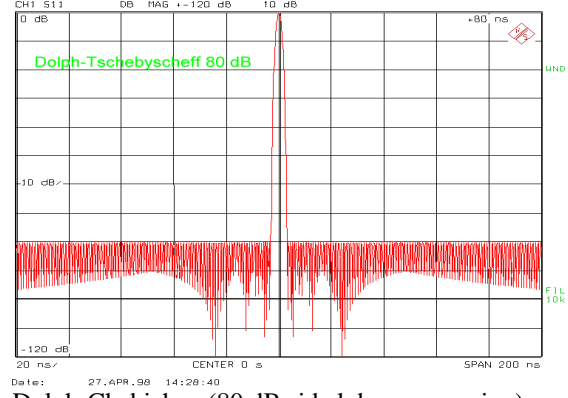
Dolph-Chebichev (40 dB side lobe suppression)



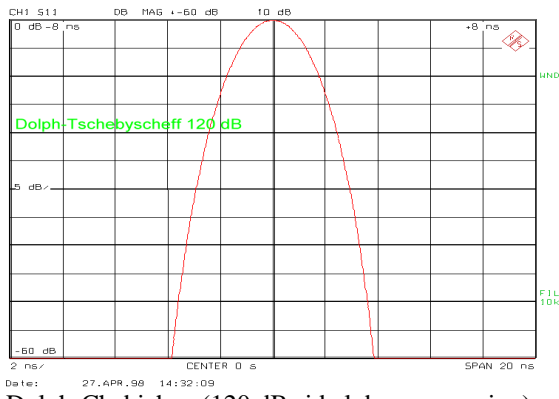
Dolph-Chebichev (40 dB side lobe suppression)



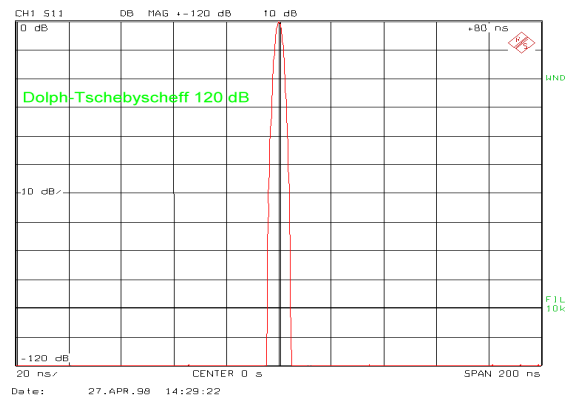
Dolph-Chebichev (80 dB side lobe suppression)



Dolph-Chebichev (80 dB side lobe suppression)

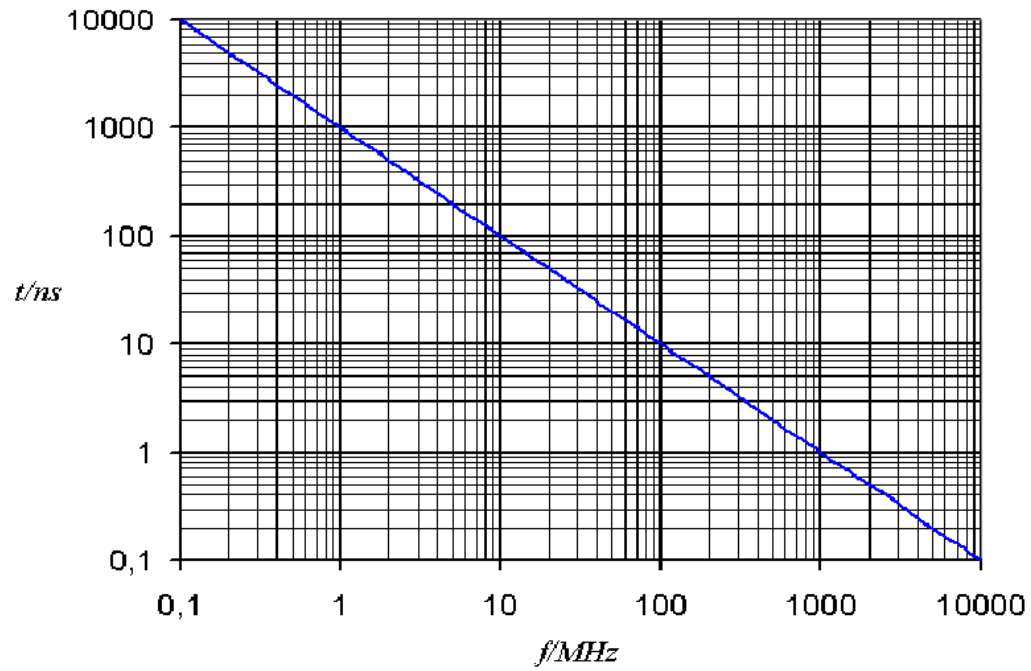


Dolph-Chebichev (120 dB side lobe suppression)



Dolph-Chebichev (120 dB side lobe suppression)

$$t = 1/f$$



Relation between step width and ambiguity range or between frequency span and pulse width.